Nanotechnology

DOI: 10.1002/anie.200906022

Diffusion-Facilitated Fabrication of Gold-Decorated Zn_2SiO_4 Nanotubes by a One-Step Solid-State Reaction**

Yang Yang, Ren Bin Yang, Hong Jin Fan, Roland Scholz, Zhipeng Huang, Andreas Berger, Yong Qin, Mato Knez, and Ulrich Gösele†*

In memory of Ulrich Gösele

Controlled incorporation of metal nanocrystallites into one-dimensional semiconductor nanostructures is expected to allow novel functionalities that go beyond those of the individual components. Design and fabrication of 1D metal–semiconductor nanocomposites, therefore, have attracted significant interest in recent years.[1] With a symmetry-breaking surface and a large surface-to-volume ratio, 1D metal–semiconductor nanocomposites can provide multiple active sites for catalysis and photoresponse. Their potential applications exist in fields ranging from new classes of catalysts to chemical sensors based on 1D nanostructures.[2]

ZnO-based ternary compounds with a composition of either ZnM_2O_4 or Zn_2MO_4 (M = Al, Si, Ga, Fe, In, Sn, Sb, Ti, Mn, V, Cr) are a family of promising multifunctional materials.[3] Most of these compounds are wide-band-gap semiconductors and typical phosphorous materials, and exhibit specific functions that are unattainable by common binary compounds. Zinc silicate (Zn_2SiO_4), with a wide band gap of 5.5 eV, has widely been used as a host material in cathode ray tubes and more recently in electroluminescent devices.[3] Zn_2SiO_4 can also serve as electronic insulator, a crystalline phase in glass ceramics, and as catalyst and catalyst support.[3] Recently, 1D Zn_2SiO_4 nanostructures, such as nanotubes and nanowires, were fabricated, and their size- and dimensionality-dependent physical and photoelectrical properties were investigated.[4] It is expected that the combination of noble metals such as gold with one-dimensional Zn_2SiO_4 nanostructures will fit specific applications. For example, owing to the electronic alignment, interactions at the Au-Zn_2SiO_4 interface are able to facilitate charge separation in Zn_2SiO_4 and further enhance energy transfer. One-dimensional Au-Zn_2SiO_4 nanocomposites could thus be utilized as chemical sensors or photocatalysts.

In general, one-dimensional metal–semiconductor hybrid nanocomposites are fabricated by overgrowth or direct attachment of metal nanocrystallites onto preformed 1D semiconductor nanostructures. Herein, a novel one-step solid-state approach is used for the fabrication of Zn_2SiO_4 nanotubes decorated with gold nanocrystallites. A controllable interfacial solid-solid reaction is performed based on a ZnO-Au-SiO_2 sandwich nanowire structure. This strategy includes contributions from the Kirkendall effect, which has extensively been used for the formation of hollow nanoobjects,[5] and a solid-state conversion process.[6] However, in contrast to previous reports, we exploit the diffusion of an interlayer (gold in this case) to influence the diffusion behavior of a thermal diffusion couple (ZnO-SiO_2). This interfacial disturbance process is important to deepen our understanding of the interdiffusion of materials on the nanoscale. Moreover, the concept developed herein can be employed as a general strategy for future fabrication of novel hybrid nanocomposites.

Single crystalline (0001)-oriented ZnO nanowires were grown by a gold-catalyzed vapor-phase transport method (see the Supporting Information for discussion and images).[7] The diameter of the ZnO nanowires is in the range of 80–150 nm; a close view reveals that the as-prepared ZnO nanowires have a quite smooth surface resulting from their well-developed crystallographic facets. A thin layer of gold was then deposited on the ZnO nanowires by sputtering, and their corresponding energy-dispersive X-ray (EDX) spectrum recorded. The morphology of the ZnO nanowires is well-preserved after the deposition of the gold film. However, their surfaces became somewhat roughened because of the non-conformal nature of the sputtering. Furthermore, we coated a 15 nm SiO_2 layer on the ZnO-Au nanowires by atomic layer deposition (ALD)[8] to obtain a ZnO-Au-SiO_2 sandwich nanowire structure. Based on both the SEM (Figure 1a) and TEM (Figure 1b) observations, we confirmed that the self-limited ALD deposition of SiO_2 formed well on the ZnO-Au nanowire substrate. The inhomogeneous contrast of the TEM image in Figure 1b indicates that the thickness of the gold interlayer around the ZnO nanowire varies from one side to another, which is due to the shadow effect of the sputtering method. However, the ALD-deposited SiO_2 shell is always uniform in thickness and conformal to the underlying undulations, even if the gold interlayer became partly

[*] Dr. Y. Yang, R. B. Yang, Dr. R. Scholz, Dr. Z. Huang, Dr. A. Berger, Dr. Y. Qin, Dr. M. Knez, Prof. U. Gösele
Max Planck Institute of Microstructure Physics
Weinberg 2, 06120 Halle (Germany)
Fax: (+49) 345-551-1223
E-mail: yangyang@mpi-halle.de

Prof. H. J. Fan
Division of Physics and Applied Physics, School of Physical and Mathematical Sciences, Nanyang Technological University
21 Nanyang Link, 637371 Singapore (Singapore)

[†] Deceased.

[**] This work was supported by the Deutsche Forschungsgemeinschaft (DFG) and the German Federal Ministry of Education and Research (BMBF: No. 03X5507).

Supporting information for this article is available on the WWW under http://dx.doi.org/10.1002/anie.200906022.

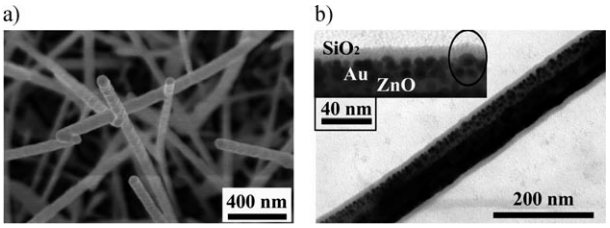

Figure 1. a) SEM and b) TEM image of ZnO-Au-SiO_2 sandwich nanowires by atomic layer deposition (ALD) of SiO_2 on gold-sputtered ZnO nanowires. Inset in (b): closer view of the sandwich nanowire structure.

discontinuous. Such a conformal deposition is clearly illustrated in the inset of Figure 1b.

The ZnO-Au-SiO_2 nanowires were subsequently annealed at 900 °C for 3 h in air. Figure 2a presents an SEM image of the product. The starting sandwich nanowires were transformed into 1D nanostructures decorated with many particles. These particles are generally less than 50 nm in size and well-distributed on the surfaces of the 1D stems (Figure 2b). TEM observations confirmed that most of the 1D nanostructures are completely hollow or composed of discontinuous long tubular sections. To determine the phase of the stems, we selected a nanotube with a relatively low nanoparticle loading to perform selected area electron diffraction (SAED) analysis (Figure 2c). The diffraction spots that were obtained exhibit the features of single crystals, and can be indexed to the rhombohedral structure of Zn_2SiO_4. Further high-resolution TEM (HRTEM) investigations (Figure 2d) revealed that the lattice fringes match those of rhombohedral Zn_2SiO_4 showing identical orientations in different areas, which is consistent with the SAED result. The Zn_2SiO_4 nanotubes are thus single crystalline in general, or at least hold a long-range single crystalline structure. Figure 2e presents the scanning TEM (STEM) image of a nanoparticle modified nanotube and the false color images of its elemental distribution. The EDX mappings indicate that Zn, Si, and O are uniformly distributed in the wall, whilst the nanoparticles consist of gold only. Therefore, the outer surface of the Zn_2SiO_4 nanotubes is decorated with gold nanocrystallites.

Based on the above results, the generation of the gold nanocrystallites decorated Zn_2SiO_4 nanotubes from the initial ZnO-Au-SiO_2 sandwich nanowires should accompany a significant outward diffusion of both the ZnO core and the gold interlayer, and also their reconfigurations. For detecting these processes, we lowered the annealing/reaction temperature. Figure 3a shows an SEM image of the sandwich nanowires annealed at 700 °C for 3 h in air, in which we can clearly observe many isolated nanoparticles encapsulated in each nanowire. TEM images (Figure 3b) verified that these particles are gold nanocrystallites disintegrated from the original gold interlayer. Most of these exhibit a tendency of departure from the ZnO-SiO_2 interface. There are no evidences for the movement of the ZnO core at this temperature. However, some visible voids in the SiO_2 shell can be observed adjacent to the core (white arrows in Figure 3b). The formation of these voids is most likely related to the

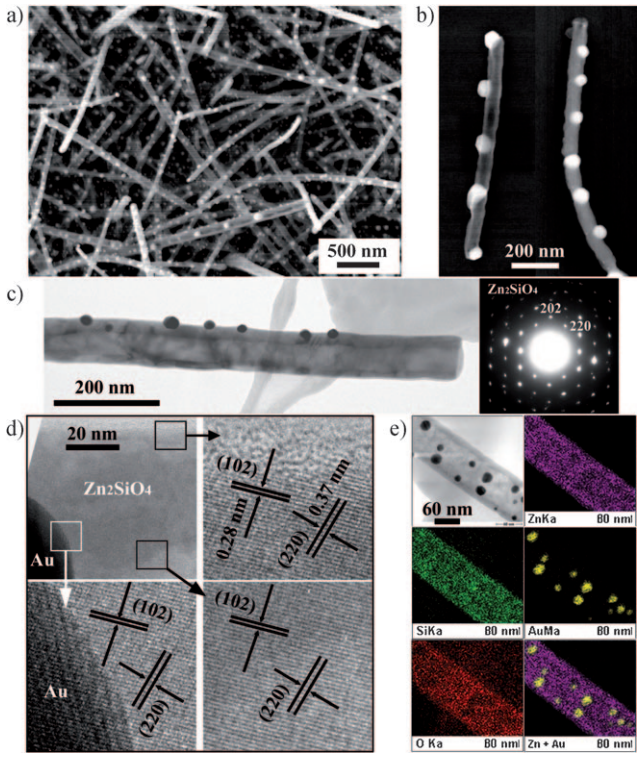

Figure 2. SEM images of one-dimensional Au/Zn_2SiO_4 nanocomposites formed by annealing ZnO-Au-SiO_2 nanowires at 900 °C for 3 h in air: a) overview, and b) close view. c) TEM image and corresponding SAED pattern of a typical Au/Zn_2SiO_4 hybrid nanotube. d) HRTEM images of three areas near a Au/Zn_2SiO_4 heterojunction. e) STEM image and corresponding EDX element mappings of Zn, Si, Au, O, and Zn + Au for one Au/Zn_2SiO_4 hybrid nanotube.

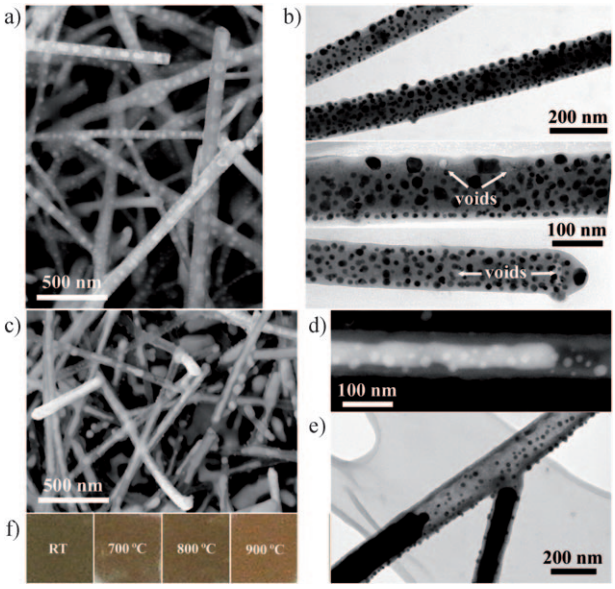

Figure 3. a) SEM and b) TEM images of one-dimensional nanostructures formed by annealing ZnO-Au-SiO_2 nanowires at 700 °C for 3 h in air. c, d) SEM and e) TEM image(s) of one-dimensional nanostructures formed by annealing ZnO-Au-SiO_2 nanowires at 800 °C for 3 h in air. f) Optical image of ZnO-Au-SiO_2 sandwich nanowire samples at room temperature and 700, 800, and 900 °C.

migration of the gold nanocrystallites along the shell. When the calcinations was carried out at 800 °C, 1D nanostructures inlaid with gold nanocrystallites started to form (Figure 3c). Many partly hollow structures appeared simultaneously (Figure 3d,e). By careful TEM analysis, we found that the tube wall of the hollow sections formed at 800 °C is composed of Zn_2SiO_4, whereas it is absent in the remaining core-shell segments (Supporting Information, Figure S2). Therefore, the formation of these tubular structures is initiated by reaction of ZnO and SiO_2 at 800 °C. An optical image (Figure 3f) shows the color of the ZnO-Au-SiO_2 sandwich nanowire samples at room temperature and after annealing at 700, 800, and 900 °C. The gradual increase of brightness with temperature also reflects the migration of gold from the initial interlayer to the final Zn_2SiO_4 nanotube outer surface.

In control experiments, ZnO-SiO_2 core–shell nanowires without a gold interlayer were prepared by the same ALD procedure (see the Supporting Information for details and images). We first annealed this sample at 800 °C for 6 h in air. In contrast to the above ZnO-Au-SiO_2 nanowire system, the product obtained at 800 °C presents only few morphological evolutions although the annealing time was doubled. In this product, several tiny cavities appeared, which probably originated from the Zn_2SiO_4-forming reaction. Further ED analysis confirmed that most ZnO nanowire cores are unaltered in this case, whereas a small quantity of superficial Zn_2SiO_4 has already been formed in some ZnO-SiO_2 core–shell nanowires. Nevertheless, the reaction rate appears to be rather sluggish compared to that of the ZnO-Au-SiO_2 sandwich nanowires; the reaction is still slow at 900 °C. Only partial core–shell nanowires were transformed into Zn_2SiO_4 nanotubes or discontinuous tubular nanostructures. Obviously, the diffusion of ZnO into the SiO_2 shell and the resultant overall reaction rate can be accelerated by the presence of the gold interlayer and its temperature-dependent migration.

Similar to the formation of $ZnAl_2O_4$ nanotubes from ZnO-Al_2O_3 core-shell nanowires, the reaction between the ZnO-SiO_2 couple involves a one-way interfacial transfer of ZnO into the SiO_2 shell, which represents an extreme case of the Kirkendall effect.[5e] With the outward diffusion of ZnO accompanying the Zn_2SiO_4 formation, a tubular structure can be formed owing to the simultaneous occurrence of a vacancy diffusion to compensate for the unequal material flow. Regarding the development of the hollow interior, it is expected that the initial stage involves the generation of small Kirkendall voids by a bulk diffusion/reaction process intersecting the ZnO-SiO_2 core–shell interface. Once these voids grow to a certain size, the remaining ZnO nanowire core will dominantly diffuse into the SiO_2 shell along the pore surface because the activation energy of the ZnO surface diffusion (158 kJ mol^{-1}) is much lower than that of its bulk diffusion (347–405 kJ mol^{-1}).[9] Therefore, the later surface diffusion of ZnO presents a faster kinetics for the void growth. In contrast, the initial nucleation of the Kirkendall voids principally determines the whole reaction rate.

TEM images of some partly evolving ZnO-SiO_2 core-shell nanowires after annealing at 900 °C in air and of ZnO-Al_2O_3 core–shell nanowires after annealing at 700 °C for comparison are given in the Supporting Information. For the ZnO-Al_2O_3 system, isolated voids distributed along the entire interface clearly show the existence of many bridge-like linkages between the residual ZnO core and the $ZnAl_2O_4$ shell.[9] This result indicates that the initial Kirkendall voids were readily nucleated all over the interface for this system. However, the heat-induced evolution of the ZnO-SiO_2 core–shell nanowires appears to be different. Distinct dividing lines were usually found in the intermediates along their axial direction; that is, the 1D nanostructures formed are composed of evolved tubular sections and unchanged core-shell segments. In particular, no voids were detected at the interface of the core–shell remainders. Based on these observations, we assume that the ZnO-SiO_2 solid–solid reaction induced by the bulk diffusion proceeded very slowly even at 900 °C. This slow reaction rate can be attributed to the high bond energy of SiO_2, but also caused by the limited supply of activated Zn^{2+} and O^{2-} ions. Therefore, an extremely long time is required for the widespread nucleation of the initial Kirkendall voids. Once a large void preferentially shaped at a weak position of the ZnO-SiO_2 interface, for example the spots with high defects or high strains, a tubular section would rapidly develop from this gap by kinetically-favored surface diffusion. Therefore, it is reasonable to suggest that the formation of the Zn_2SiO_4 nanotubes from the ZnO-SiO_2 core–shell nanowires is actually triggered by a few preferentially generated interfacial voids rather than a randomly distributed void evolution at the ZnO-SiO_2 interface.

When a gold interlayer was present at the ZnO-SiO_2 core–shell interface, the migration of gold nanocrystallites in and through the SiO_2 shell occurred during the annealing process. External forces, such as heat or an electron beam, can induce the transport of gold particles in a thin SiO_2 film.[10] The transport process is explained by a wetting process followed by the Stokes motion of a solid sphere in a viscous medium. In our case, heat first induced the disintegration of the gold interlayer into isolated nanocrystallites at the ZnO-SiO_2 interface. These nanocrystallites then gradually migrated from the interface to the outer surface of the SiO_2 shell. The driving force for the motion should be the reduction in interface energy upon successive replacement of the interface ZnO-Au-SiO_2 by the Au-SiO_2 and the SiO_2-Au-air interfaces. During the migration, surface diffusion of SiO_2 along the gold nanocrystallites took place, which filled the gold-vacated spaces in the shell. Furthermore, some small gold nanocrystallites might have grown larger owing to their collision and to Ostwald ripening.

As the fluidity of solid state SiO_2 is limited at temperatures far below its melting point, it is supposed that some vacancies induced by the motion of the gold nanocrystallites failed to be timely compensated. These frozen vacancies would possibly fuse into large voids during annealing, some of which gathered at the ZnO-SiO_2 core-shell interface, as confirmed by our observations (Figure 3b). Moreover, the surface diffusion of SiO_2 along different gold nanocrystallites resulted in an unequal thermal reconfiguration of the initial ALD-deposited SiO_2 shell. Abundant defects and weakened bonds would be produced in the interfacial SiO_2 in contrast to the annealing process without the gold interlayer. Therefore,

it can be inferred that the gold motion introduced additional voids, vacancies, and defects into the ZnO-SiO_2 nanowire interface, which facilitated the nucleation of the Kirkendall voids at multiple positions by bulk diffusion. Once this initial void nucleation was adequately achieved, the ZnO nanowire core could rapidly diffuse into the SiO_2 shell along the interfacial void surfaces. Therefore, the formation of a Zn_2SiO_4 nanotube was accelerated. As for ZnO nanowires with large diameters, excess ZnO was likely to further diffuse along the void surface toward the Zn_2SiO_4 wall and desorb on its outer surface.[4d,11] The above procedures proposed for the formation of the gold-decorated Zn_2SiO_4 nanotubes are shown in Scheme 1.

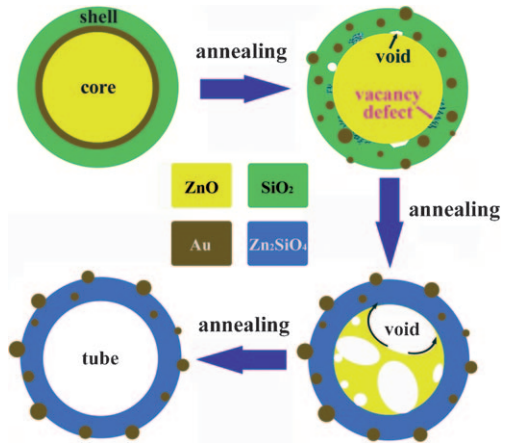

Scheme 1. The growth process for Zn_2SiO_4 nanotubes decorated with gold nanocrystallites and formed from ZnO-Au-SiO_2 sandwich nanowires by annealing at high temperatures. (The shadow effect during the sputtering of gold is not shown).

According to this growth mode, decoration of the gold nanocrystallites on the Zn_2SiO_4 nanotubes was derived from a gradual extraction from the interior instead of a loose attachment to the exterior. As a result, the gold nanocrystallites could be inlaid into the nanotube wall with a suitable annealing time. From the images shown in Figure 4, it can be clearly seen that the gold nanocrystallites are indeed anchored into respective valleys on the outer wall of the nanotube by this one-step solid–solid reaction. To make a comparison, we directly sputtered a gold layer with the same thickness on the ZnO nanowires, and then annealed this sample at 900 °C for 3 h in air. In this case, the starting gold film was finally transformed into very large particles owing to wetting and serious aggregations at high temperatures (Supporting Information, Figure S5a). This difference indicates that the size evolution of the gold nanocrystallites can be obviously restrained owing to the steric barrier provided by this embedded structure even at 900 °C and the duration of 3 h. This effective size control is of advantage especially when this Au-Zn_2SiO_4 hybrid composite is employed as high-temperature catalysts. The gold loading for a SiO_2 shell with certain thickness is limited: when a much thicker gold interlayer was sandwiched between the ZnO nanowire core and the 15 nm SiO_2 shell, most gold particles migrating from the interior were forced to break away from the final product after annealing under the same conditions (Supporting Information, Figure S5b). The tubular structure of Zn_2SiO_4 also cracked and collapsed. Thus, the formation of perfect Zn_2SiO_4 nanotubes decorated with size-controllable gold nanocrystallites is strongly dependent on the thickness of the gold interlayer involved.

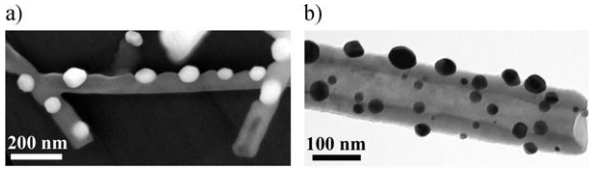

Figure 4. a) SEM and b) TEM image of Zn_2SiO_4 nanotubes decorated with gold nanocrystallites prepared by annealing ZnO-Au-SiO_2 nanowires at 900 °C for 3 h in air. The images verify that the gold nanocrystallites are inlaid in the nanotube wall.

In summary, a one-step solid-state approach for the fabrication of Zn_2SiO_4 nanotubes decorated with gold nanocrystallites has been presented. This fabrication strategy is based on a ZnO-Au-SiO_2 sandwich nanowire structure, in which a thin gold interlayer is intentionally incorporated. The Zn_2SiO_4 nanotubes are formed by a one-way interfacial transfer of the ZnO core into the SiO_2 shell at high temperatures and induced by the Kirkendall effect. The gold interlayer has two functions: first, it is the gold precursor, which can transform into gold nanocrystallites and further migrate to the outer surface of the SiO_2 shell during the annealing process. Second, the heat-driven motion of the gold interlayer can influence the ZnO-SiO_2 core-shell interface by facilitating the initial nucleation of the Kirkendall voids and accelerating the formation of the Zn_2SiO_4 nanotubes. The gold-decorated Zn_2SiO_4 nanotubes obtained present a stable nanocomposite structure. The strategy developed herein is also expected to be used as a general route for the fabrication of novel hybrid nanocomposites in the future.

Received: October 26, 2009
Published online: January 22, 2010

Keywords: core–shell materials · gold · interfacial reactions · nanotubes · solid-state structures

[1] a) J. Luo, L. Zhang, Y. J. Zhang, J. Zhu, *Adv. Mater.* **2002**, *14*, 1413; b) T. Mokari, E. Rothenberg, I. Popov, R. Costi, U. Banin, *Science* **2004**, *304*, 1787; c) T. Mokari, C. G. Sztrum, A. Salant, E. Rabani, U. Banin, *Nat. Mater.* **2005**, *4*, 855; d) A. J. Mieszawska, R. Jalilian, G. U. Sumanasekera, F. P. Zamborini, *Small* **2007**, *3*, 722; e) I. Jen-La Plante, S. E. Habas, B. D. Yuhas, D. J. Gargas, T. Mokari, *Chem. Mater.* **2009**, *21*, 3662.

[2] a) Y. Wu, J. Xiang, C. Yang, W. Lu, C. M. Lieber, *Nature* **2004**, *430*, 61; b) R. Z. Ma, T. Sasaki, Y. Bando, *J. Am. Chem. Soc.* **2004**, *126*, 10382; c) J. Lee, A. O. Govorov, J. Dulka,, N. A. Kotov, *Nano Lett.* **2004**, *4*, 2323; d) A. Kolmakov, D. O. Klenov, Y. Lilach, S. Stemmer, M. Moskovits, *Nano Lett.* **2005**, *5*, 667; e) W. Lim, J. S. Wright, B. P. Gila, J. L. Johnson, A. Ural, T. Anderson, F. Ren, S. J. Pearton, *Appl. Phys. Lett.* **2008**, *93*, 072109.

[3] H. J. Fan, Y. Yang, M. Zacharias, *J. Mater. Chem.* **2009**, *19*, 885.
[4] a) X. D. Wang, C. J. Summers, Z. L. Wang, *Adv. Mater.* **2004**, *16*, 1215; b) X. Feng, X. Yuan, T. Sekiguchi, W. Lin, J. Kang, *J. Phys. Chem. B* **2005**, *109*, 15786; c) J. Wang, J. Ge, H. Zhang, Y. Li, *Small* **2006**, *2*, 257; d) J. Zhou, J. Liu, X. Wang, J. Song, R. Tummala, N. S. Xu, Z. L. Wang, *Small* **2007**, *3*, 622; e) H. Q. Wang, G. Z. Wang, L. C. Jia, C. J. Tang, G. H. Li, *J. Phys. Chem. C* **2007**, *111*, 14307; f) B. Cheng, X. Yu, H. Liu, Z. Wang, *J. Phys. Chem. C* **2008**, *112*, 16312.
[5] a) A. D. Smigelskas, E. O. Kirkendall, *Trans. Am. Inst. Min. Eng.* **1947**, *171*, 130; b) Y. Yin, R. M. Rioux, C. K. Erdonmez, S. Hughes, G. A. Somorjai, A. P. Alivisatos, *Science* **2004**, *304*, 711; c) Q. Li, R. M. Penner, *Nano Lett.* **2005**, *5*, 1720; d) Y. Wang, L. Cai, Y. Xia, *Adv. Mater.* **2005**, *17*, 473; e) H. J. Fan, M. Knez, R. Scholz, K. Nielsch, E. Pippel, D. Hesse, M. Zacharias, U. Gösele, *Nat. Mater.* **2006**, *5*, 627; f) S. Peng, S. Sun, *Angew. Chem.* **2007**, *119*, 4233; *Angew. Chem. Int. Ed.* **2007**, *46*, 4155; g) H. J. Fan, U. Gösele, M. Zacharias, *Small* **2007**, *3*, 1660; h) Y. Yang, D. S. Kim, R. Scholz, M. Knez, S. M. Lee, U. Gösele, M. Zacharias, *Chem. Mater.* **2008**, *20*, 3487; i) K. An, T. Hyeon, *Nano Today* **2009**, *4*, 359.
[6] a) K. Jacobs, D. Zaziski, E. C. Scher, A. B. Herhold, A. P. Alivisatos, *Science* **2001**, *293*, 1803; b) U. Jeong, P. H. C. Camargo, Y. H. Lee, Y. Xia, *J. Mater. Chem.* **2006**, *16*, 3893; c) M. J. Bierman, K. M. Van Heuvelen, D. Schmeißer, T. C. Brunold, S. Jin, *Adv. Mater.* **2007**, *19*, 2677.
[7] H. J. Fan, B. Fuhrmann, R. Scholz, C. Himcinschi, A. Berger, H. Leipner, A. Dadgar, A. Krost, S. Christiansen, U. Gösele, M. Zacharias, *Nanotechnology* **2006**, *17*, S231.
[8] J. Bachmann, R. Zierold, Y. T. Chong, R. Hauert, C. Sturm, R. Schmidt-Grund, B. Rheinlnder, M. Grundmann, U. Gösele, K. Nielsch, *Angew. Chem.* **2008**, *120*, 6272; *Angew. Chem. Int. Ed.* **2008**, *47*, 6177.
[9] a) H. J. Fan, M. Knez, R. Scholz, D. Hesse, K. Nielsch, M. Zacharias, U. Gösele, *Nano Lett.* **2007**, *7*, 993; b) Y. Yang, D. S. Kim, M. Knez, R. Scholz, A. Berger, E. Pippel, D. Hesse, U. Gösele, M. Zacharias, *J. Phys. Chem. C* **2008**, *112*, 4068.
[10] J. Biskupek, U. Kaiser, F. Falk, *J. Electron Microsc.* **2008**, *57*, 83.
[11] a) Y. Yang, R. Scholz, A. Berger, D. S. Kim, M. Knez, D. Hesse, U. Gösele, M. Zacharias, *Small* **2008**, *4*, 2112; b) H. J. Fan, A. Lotnyk, R. Scholz, Y. Yang, D. S. Kim, E. Pippel, S. Senz, D. Hesse, M. Zacharias, *J. Phys. Chem. C* **2008**, *112*, 6770; c) Y. Yang, R. Scholz, H. J. Fan, D. Hesse, U. Gösele, M. Zacharias, *ACS Nano* **2009**, *3*, 555.

